Hydrogen sulfide (H_2S) metabolism in mitochondria and its regulatory role in energy production

Ming Fu[a,1], Weihua Zhang[b,c,1], Lingyun Wu[b,c], Guangdong Yang[d], Hongzhu Li[a,c], and Rui Wang[a,2]

[a]Department of Biology and [d]School of Kinesiology, Lakehead University, Thunder Bay, ON, Canada P7B 5E1; [b]Department of Pharmacology, University of Saskatchewan, Saskatoon, SK, Canada S7N 5E5; and [c]Department of Pathophysiology, Harbin Medical University, Harbin 150086, China

Edited* by Solomon H. Snyder, The Johns Hopkins University School of Medicine, Baltimore, MD, and approved January 10, 2012 (received for review September 22, 2011)

Although many types of ancient bacteria and archea rely on hydrogen sulfide (H_2S) for their energy production, eukaryotes generate ATP in an oxygen-dependent fashion. We hypothesize that endogenous H_2S remains a regulator of energy production in mammalian cells under stress conditions, which enables the body to cope with energy demand when oxygen supply is insufficient. Cystathionine γ-lyase (CSE) is a major H_2S-producing enzyme in the cardiovascular system that uses cysteine as the main substrate. Here we show that CSE is localized only in the cytosol, not in mitochondria, of vascular smooth-muscle cells (SMCs) under resting conditions, revealed by Western blot analysis and confocal microscopy of SMCs transfected with GFP-tagged CSE plasmid. After SMCs were exposed to A23187, thapsigargin, or tunicamycin, intracellular calcium level was increased, and CSE translocated from the cytosol to mitochondria. CSE was coimmunoprecipitated with translocase of the outer membrane 20 (Tom20) in mitochondrial membrane. *Tom20* siRNA significantly inhibited mitochondrial translocation of CSE and mitochondrial H_2S production. The cysteine level inside mitochondria is approximately three times that in the cytosol. Translocation of CSE to mitochondria metabolized cysteine, produced H_2S inside mitochondria, and increased ATP production. Inhibition of CSE activity reversed A23187-stimulated mitochondrial ATP production. H_2S improved mitochondrial ATP production in SMCs with hypoxia, which alone decreased ATP production. These results suggest that translocation of CSE to mitochondria on specific stress stimulations is a unique mechanism to promote H_2S production inside mitochondria, which subsequently sustains mitochondrial ATP production under hypoxic conditions.

mitochondrion | oxygen sensing | evolution | sulfur metabolism | phenylephrine

Many photoautotrophic and chemoautotrophic bacteria and certain animals, such as the lugworm *Arenicola marina*, use sulfide as an energetic substrate. Mitochondria are the powerhouse of eukaryotic cells, where ATP is produced via oxidative phosphorylation. Considering mitochondria as the evolutionary trait of bacteria in eukaryotes, the metabolism of hydrogen sulfide (H_2S) in mitochondria may serve as a means for energy supplementation. It has been demonstrated that H_2S can drastically reduce metabolic demand (1). Similar to nitric oxide, H_2S exerts protective effects on mitochondrial function and respiration (2). However, a conventional belief is that H_2S is produced in the cytoplasm resulting from the cytosol localization of H_2S-generating enzymes and is consumed through oxidation in mitochondria (3). It was recently demonstrated that mitochondria of human colon adenocarcinoma cells use sulfide as an energetic substrate at low micromolar concentrations, well below toxic levels (4). The foregoing observations call for reevaluation of the metabolism of H_2S and its role in mitochondrial energization of eukaryotes. In the present study, we explored whether H_2S can be produced inside mitochondria and if so, the underlying mechanisms of this production. We also examined the correlation of mitochondrial production of H_2S and oxygen-dependent ATP production.

Results

Mitochondrial Localization of Cystathionine γ-Lyase and Production of H_2S. Under resting conditions, cystathionine γ-lyase (CSE) proteins were detectable in the whole-cell preparation, but not in the mitochondrial fraction, from wide-type (WT) smooth muscle cells (SMCs) (Fig. 1*A*). In SMCs from CSE knockout (KO) mice, no CSE band was detected in the whole cell preparation. After cell incubation with 2 μM A23187, CSE proteins were detectable in WT-SMC mitochondria (Fig. 1*A*). The appearance of CSE protein in mitochondria was obvious at 16 h after A23187 stimulation and remained so over the 48 h of the experiment (Fig. 1*B*). Moreover, CSE translocation into mitochondria was A23187 concentration-dependent (Fig. 1*C*). A23187-induced CSE mitochondrial translocation is related to increased intracellular calcium level, and it was inhibited by 43.3 ± 12.2% with 1,2-bis(o-aminophenoxy)ethane-*N*,*N*,*N*′,*N*′-tetraacetic acid (BAPTA) and by 45.3 ± 15.8% with EGTA (Fig. 1*D*). BAPTA or EGTA alone did not induce mitochondrial translocation of CSE (Fig. S1*A*).

To follow the intracellular trafficking of CSE, we transfected WT-SMCs with pCSE-GFP or AcGFP1-N1. Successful transfection with pCSE-GFP was detected by Western blot analysis with an anti-GFP antibody and identified as a 70-kDa product, which is the predicted size of the GFP-tagged CSE (Fig. 1*E*). Confocal fluorescence microscopy confirmed that under resting conditions, no GFP-tagged CSE was present in mitochondria. After the cells were treated with A23187, the green image of GFP-tagged CSE merged with the red image of mitochondrial marker (Fig. 1*F*), confirming CSE translocation into the mitochondria.

Translocase of the Outer Membrane 20-Mediated CSE Mitochondrial Translocation. To identify the transport machinery for CSE translocation, we determined the expression profile of translocase of the outer membrane 20 (Tom20). Tom20 was identified in mitochondria isolated from WT-SMCs, and its expression was increased by A23187 (Fig. 2*A*). After A23187 stimulation, mitochondrial CSE translocation occurred, and CSE was coprecipitated with Tom20 (Fig. 2*B*). Given that antibodies against CSE and Tom20 are derived from rabbits, rabbit IgGs were used as a blank in coimmunoprecipitation. Tom20 expression levels were the same in WT-SMCs and KO-SMCs. DL-propargylglycine (PPG) treatment of WT-SMCs did not alter Tom20 expression level (Fig. S1*B*). In contrast, A23187 treatment of WT-SMCs and KO-SMCs increased Tom20 expression (Fig. S1*C*). Together, these data show that the increased Tom20 expression after A23187 is not secondary to altered CSE translocation or activity.

Author contributions: L.W., G.Y., and R.W. designed research; M.F., W.Z., and H.L. performed research; M.F., W.Z., L.W., G.Y., and R.W. analyzed data; and L.W. and R.W. wrote the paper.

The authors declare no conflict of interest.

*This Direct Submission article had a prearranged editor.

[1]M.F. and W.Z. contributed equally to this work.

[2]To whom correspondence should be addressed. E-mail: rwang@lakeheadu.ca.

This article contains supporting information online at www.pnas.org/lookup/suppl/doi:10.1073/pnas.1115634109/-/DCSupplemental.

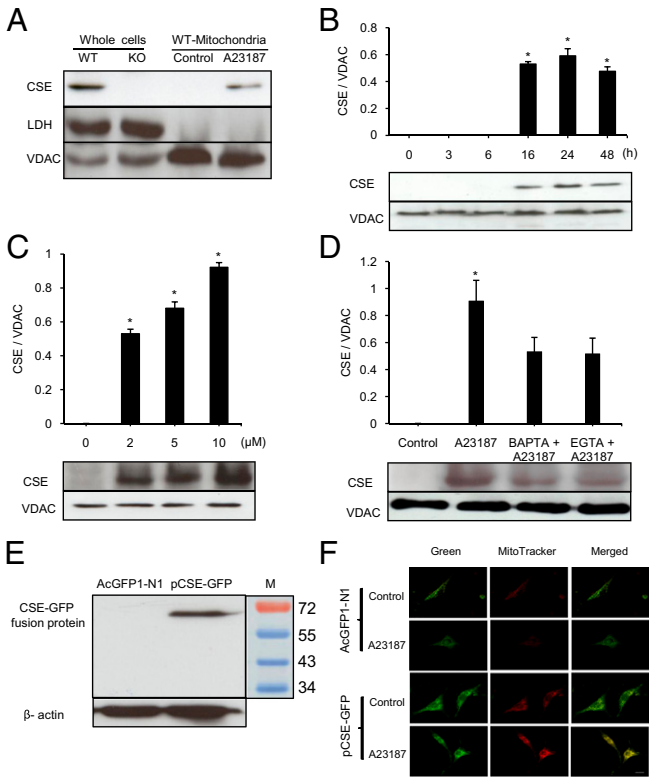

Fig. 1. A23187-induced CSE mitochondrial translocation. (*A*) Western blot analysis of A23187- induced CSE mitochondrial translocation. Samples from KO-SMCs were used as negative control. Lactate dehydrogenase (LDH) and voltage-dependent anion channel (VDAC) served as the cytosolic and mitochondrial markers, respectively ($n = 6$). (*B*) Time-dependent translocation of CSE into mitochondria induced by treatment with 2 μM A23187 ($n = 4$; $^*P <$ 0.05 vs. control). (*C*) Concentration-dependent effect of A23187 on CSE mitochondrial translocation after 24 h of treatment ($n = 4$; $^*P < 0.05$ vs. control). (*D*) Inhibitory effects of BAPTA (100 μM) and EGTA (1 mM) on A23187-induced CSE mitochondrial translocation ($n = 4$; $^*P < 0.05$ vs. all other groups). (*E*) Western blot analysis of GFP-tagged CSE expression in transfected WT-SMCs ($n = 3$). (*F*) Confocal immunofluorescence analysis of CSE-GFP expression in transfected WT-SMCs. MitoTracker Red CMXRos (red) indicates the location of mitochondria, and the location of CSE-GFP is shown in green. Yellow images reflect the overlapped mitochondria and CSE-GFP colocalization. (Scale bar, 20 μm.) The images in the panels are representative examples.

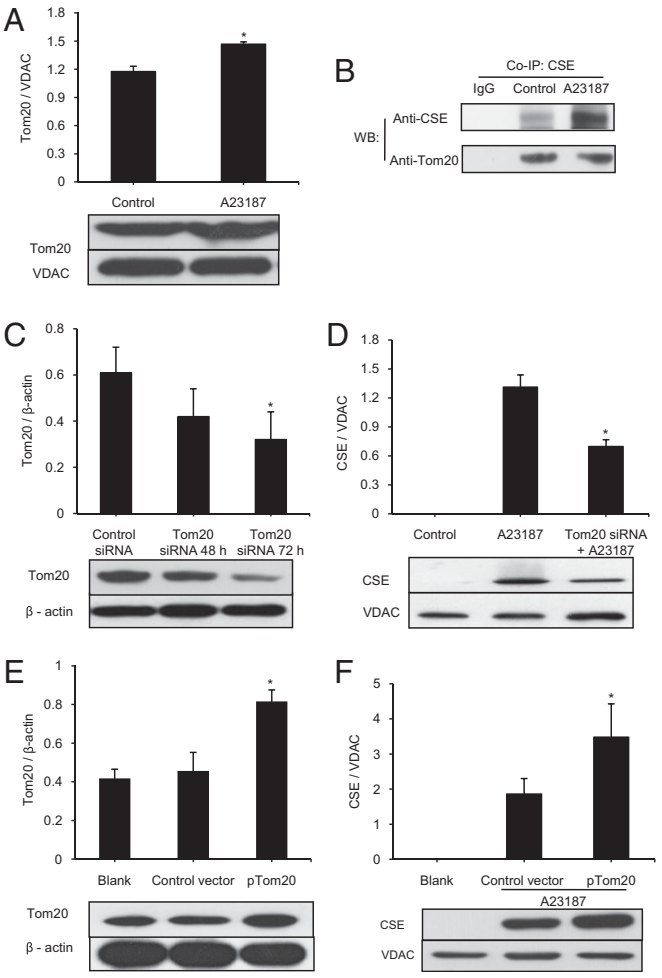

Fig. 2. Involvement of Tom20 in A23187-induced CSE mitochondrial translocation. (*A*) Effect of A23187 incubation for 24 h on mitochondrial Tom20 expression ($n = 4$; $^*P < 0.05$). (*B*) Coimmunoprecipitation (Co-IP) analyses of the interactions between CSE and Tom20. In Co-IP with anti-Tom20 polyclonal antibody, the protein complex from Co-IP was immunoprecipitated and analyzed by Western blotting with the indicated antibodies ($n = 5$). (*C*) Effects of *Tom20* siRNA and control-siRNA on Tom20 protein expression by Western blot analysis ($n = 4$; $^*P < 0.05$ vs. other groups). (*D*) Effect of *Tom20* siRNA on mitochondrial translocation of CSE protein, detected by Western blot analysis. The cells were first transfected with 100 nM *Tom20*-siRNA for 72 h, after which 2 μM A23187 was added for another 24 h ($n = 4$; $^*P < 0.05$ vs. other groups). (*E* and *F*) Western blot analysis of Tom20 overexpression (*E*) and its effect on mitochondrial CSE translocation stimulated by 2 μM A23187 for 24 h, with pcDNA3.1(+) applied as control vector (*F*) ($n = 4$; $^*P < 0.05$). The images in the panels are representative examples.

To confirm a mediating role of Tom20 for CSE importation into mitochondria, we applied *Tom20* siRNA to transfect WT-SMCs. Transfection with *Tom20* siRNA for 72 h resulted in a 44.8 ± 11.8% reduction of Tom20 expression (Fig. 2*C*). A23187-induced mitochondrial translocation of CSE in *Tom20* siRNA-transfected cells was decreased by 46.8 ± 8.9% compared with that without *Tom20* knockdown (Fig. 2*D*). We also overexpressed Tom20 in WT-SMCs by transfecting the cells with pTom20 for 72 h. This transfection resulted in 95.4 ± 11.6% increase in Tom20 expression compared with untreated blank (Fig. 2*E*). Coincidently, the amount of A23187-stimulated CSE translocation into mitochondria with overexpressed Tom20 increased by 87.4 ± 32.7% compared with transfection with the control vector (Fig. 2*F*).

Along with promoting mitochondrial translocation of CSE, A23187 treatment also up-regulated the expression of CSE. After WT-SMCs were incubated with 2 μM A23187 for 24 h, CSE protein content was increased by 182.5 ± 28.4% compared with the control group (Fig. 3*A*). A23187-stimulated CSE mRNA overexpression was significantly attenuated by pretreatment of the cells with EGTA or BAPTA for 30 min (Fig. 3*B*).

To assay whether mitochondrial CSE translocation also could be triggered by other stimuli, phenylephrine (5 μM), thapsigargin (1 μM), and tunicamycin (5 μg/mL) were applied to cells. All three of these agents increased intracellular Ca^{2+} (Fig. 3*C*); however, the kinetics of calcium changes with the different stimuli differed significantly. The increase in intracellular Ca^{2+} level reached a peak at 37.7 ± 7 s after the application of A23187, 35.2 ± 3.4 s after the application of thapsigargin, and 29.5 ± 3.2 s after the application of tunicamycin ($n = 4$ for each group), but at only 3.2 ± 0.6 s after the application of phenylephrine ($n = 4$). Moreover, within 30 s, the effect of phenylpherine on intracellular calcium subsided, but the effects of A23187, thapsigargin, and tunicamycine persisted during the observation period (Fig. 3*C*).

Mitochondrial CSE translocation was detected in the presence of thapsigargin and tunicamycine (Fig. 3*D* and Fig. S1*D*), but not

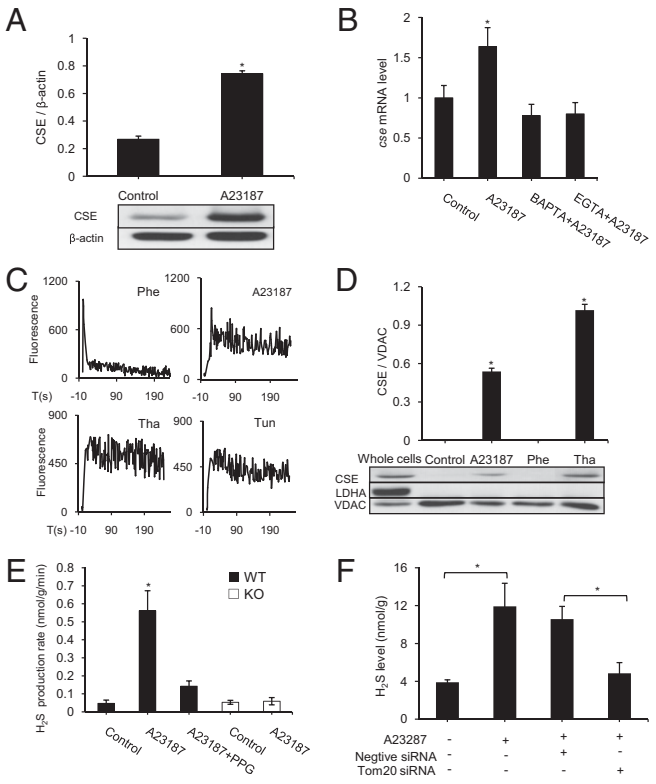

Fig. 3. Regulation of mitochondrial CSE translocation and H_2S production in WT-SMCs. (*A*) Western blot analysis of CSE protein content in whole cell lysate ($n = 3$; $^*P < 0.05$). Representative Western blot images are shown. (*B*) Real-time PCR analysis of *cse* mRNA expression level after 24 h of treatment with A23187 in the presence of BAPTA (100 μM) or EGTA (1 mM) ($n = 4$; $^*P < 0.05$ vs. all other groups). (*C*) Changes in intracellular calcium levels in WT-SMCs observed with Fluo4-AM. Different agents were added to the culture medium at time 0. ($n = 4$ for each group). (*D*) Effects of A23187 (2 μM), phenylephrine (Phe; 5 μM), and thapsigargin (Tha; 1 μM) on CSE mitochondrial translocation detected by Western blot analysis ($n = 4$; $^*P < 0.05$ vs. control). (*E*) H_2S production rate of the sonicated mitochondrial fractions of WT-SMCs and KO-SMCs with or without treatment with A23187 (2 μM) and PPG (5 mM) ($n = 5$; $^*P < 0.05$ vs. other groups). (*F*) Effect of *Tom20* siRNA on mitochondrial H_2S concentrations of the intact mitochondria without sonication in the presence of 2 μM A23187 for 24 h ($n = 4$; $^*P < 0.05$).

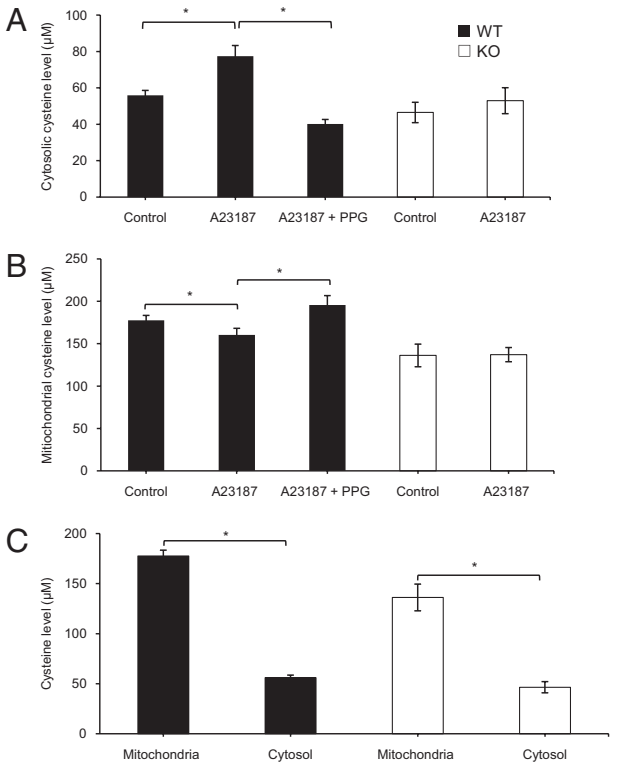

Fig. 4. Changes in cysteine levels in the cytosol and mitochondria. (*A*) A23187- (2 μM) induced increase in cytosolic cysteine level in WT-SMCs and KO-SMCs ($n = 4$; $^*P < 0.05$ vs. other groups). (*B*) Effect of 2 μM A23187 on mitochondrial cysteine level in WT-SMCs and KO-SMCs ($n = 4$; $^*P < 0.05$). (*C*) Differences in cysteine levels between cytosol and mitochondria of WT-SMCs and KO-SMCs ($n = 4$; $^*P < 0.05$ vs. cytosolic cysteine level).

in the presence of phenylephrine (Fig. 3*D*), H_2O_2 (100 μM) or LPS (2 μg/mL) (Fig. S2*B*). The inhibition of endoplasmic reticulum (ER) stress with 4-phenylbutyrate (4-PBA) decreased the transcriptional expression of *atf4*, an ER stress marker (5), which was first up-regulated by A23187, thapsigargin, and tunicamycin (Fig. S2*A*). However, 4-PBA did not affect CSE mitochondrial translocation induced by A23187, thapsigargin, or tunicamycin (Fig. S1*D*). Mitochondrial CSE translocation also appears to be cell type-specific. A23187 did not cause CSE translocation into mitochondria in WiDr cells, a colon adenocarcinoma line, although those cells express CSE in their cytoplasm (Fig. S2*C*).

H_2S production rate in the A23187-treated WT-SMC mitochondrial fractions was significantly increased compared with nontreated control samples, and this effect was inhibited by 5 mM PPG, a CSE inhibitor. In sharp contrast, A23187 challenge did not alter mitochondrial H_2S production in KO-SMCs (Fig. 3*E*). Knockdown of *Tom20* with *Tom20* siRNA significantly decreased A23187-induced endogenous production of H_2S from the intact mitochondria (Fig. 3*F*). These data indicate that A23187-stimulated H_2S production in mitochondria is related to the specific catalytic activity of CSE that translocates from the cytosol to mitochondrion.

Mitochondrial Translocation of CSE Is Important for Mitochondrial Cysteine Metabolism. A23187 (2 μM) stimulation of WT-SMCs for 24 h increased cytosolic cysteine level by 38.5 ± 3.5% compared with the untreated group (Fig. 4*A*). In contrast, A23187 treatment of WT-SMCs decreased mitochondrial cysteine content by 18.8 ± 3.4% compared with the untreated group (Fig. 4*B*). Both the A23187-induced increase in cytosolic cysteine level and the decrease in mitochondrial cysteine level were abolished by 5 mM PPG. In KO-SMCs, A23187 had no significant effects on either cytosolic or mitochondrial cysteine level (Fig. 4 *A* and *B*). Mean mitochondrial cysteine levels in WT-SMCs (177.5 ± 5.8 μM) and KO-SMCs (136.2 ± 13.4 μM) were approximately threefold those in cytosolic fractions (Fig. 4*C*).

Effect of CSE Mitochondrial Translocation on Energy Metabolism. To test the impact of CSE mitochondrial translocation on energy metabolism, we exposed WT-SMCs to 2 μM A23187 for 24 h under normoxic conditions to induce CSE translocation. This treatment resulted in elevated ATP content, which was partially but significantly blocked by PPG (Fig. 5*A*). The same A23187 treatment of KO-SMCs also increased mitochondrial ATP production, but to a significantly lower degree than in WT-SMCs, and it could not be blocked by PPG (Fig. 5*A*). Under hypoxic conditions, A23187 treatment increased ATP production only in WT-SMCs, not in KO-SMCs (Fig. 5*B*), indicating that mitochondrial translocation of CSE is solely responsible for the A23187-induced ATP production in hypoxia. NaHS (0.01–100 μM), a H_2S donor, caused a concentration-dependent decrease in ATP content under normoxic condition but increased ATP production under hypoxic conditions (Fig. 5*C*). The NaHS-stimulated ATP production under hypoxic condition was also observed in intact WT-

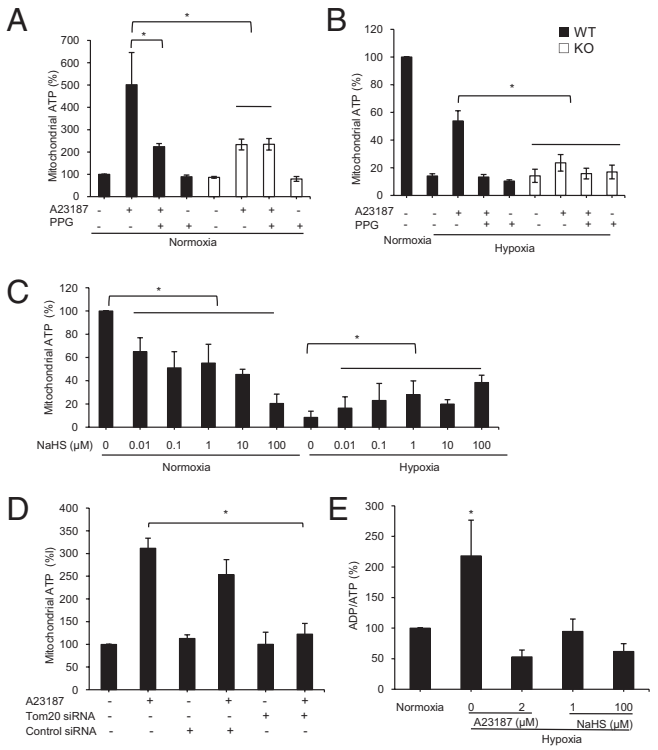

Fig. 5. Effects of endogenous and exogenous H_2S on mitochondrial ATP production. (*A*) Effect of A23187 (2 μM) on mitochondrial ATP production in the presence or absence of 5 mM PPG in WT-SMCs and KO-SMCs under normoxic conditions (n = 8). (*B*) Effect of A23187 (2 μM) on mitochondrial ATP production in the presence or absence of 5 mM PPG in WT-SMCs and KO-SMCs under hypoxic conditions (n = 4). (*C*) Interaction of H_2S and O_2 on mitochondrial ATP production in WT-SMCs (n = 4). (*D*) Effect of Tom20 knockdown with Tom20 siRNA on ATP production in WT-SMCs (n = 4). (*E*) Interaction of H_2S and O_2 on mitochondrial ADP/ATP ratio in WT-SMCs (n = 4 for each group). *P < 0.05 for all panels.

SMCs (Fig. S2*D*). Knockdown of *Tom20* expression abolished A23187-induced ATP production (Fig. 5*D*), further supporting the role of Tom-20-mediated CSE translocation in the effect of A23187. The ADP/ATP ratio, a value that reflects the state of mitochondrial ATP production, was significantly increased in mitochondria under hypoxic condition, but this increase was reversed by both A23187 and NaHS (Fig. 5*E*).

Discussion

Certain types of bacteria and archae contain specific enzymes that provide H_2S as the energy substrate. Analysis of the universal phylogenetic tree (maps that link the beginning of life on Earth to modern-day life) based on small-subunit rRNA sequences of the organisms represented indicates that almost all life on Earth may share the same universal ancestor, and that some common genetic traits may be passed on down the phylogenetic tree. The use of molecular phylogenetic techniques has led to an initial assumption that mammalian cells (branch of Eucarya) also may be equipped with machinery to produce and use H_2S (6), especially considering that mitochondria in eukaryotes are evolutionally related to bacteria. The mitochondrial genome in eukaryotes does not include genetic code for H_2S-generating enzymes, however. This difference between bacteria and eukaryote mitochondria of eukaryotes may indicate that the need for H_2S to regulate energy metabolism has not been reserved during evolution; however, this notion has not been postulated or tested. The present study provides evidence that H_2S can be produced inside mitochondria after CSE is translocated into mitochondria, and that mitochondrial H_2S is involved in the regulation of mitochondrial energy metabolism. As such, the conventional thinking regarding the regulation of eukaryote mitochondrial function, compared with that of bacteria, should be revised.

The intracellular localization of CSE in SMCs has not been critically determined. Our data show that under resting conditions, CSE expression and H_2S production are confined in the cytosol of SMCs, not in mitochondria. On stimulation with the calcium ionophore A23187, CSE translocates from the cytosol into mitochondria, and H_2S is now produced inside mitochondria. The promotion of CSE translocation by A23187 is due to an increased intracellular calcium level ($[Ca^{2+}]_i$). Chelating extracellular calcium with EGTA or intracellular free calcium with BAPTA significantly inhibits the effect of A23187 on CSE translocation.

Phenylephrine, thapsigargin, and tunicamycin also increase $[Ca^{2+}]_i$ via different mechanisms. Only in the presence of thapsigargin and tunicamycin is CSE translocated into mitochondria. Thapsigargin increases $[Ca^{2+}]_i$ by releasing Ca^{2+} from the ER via inhibition of the sarco(endo)plasmic reticulum Ca^{2+}-ATPase (1, 7, 8). Thapsigargin also may affect protein and DNA synthesis, DNA fragmentation apoptosis (9), and ER stress (10). Tunicamycin is a well-known ER stress inducer that acts by blocking *N*-glycosylation of newly synthesized proteins (11). Thapsigargine, tunicamycin, and A23187 share the ability to enhance $[Ca^{2+}]_i$ as well as induce ER stress (10, 12), whereas phenylephrine does not affect ER stress (13). Therefore, we further tested whether the increased ER stress was the cause of CSE mitochondrial translocation. Our results show that the inhibition of ER stress with 4-PBA (5) had no effect on CSE translocation induced by A23187, thapsigargin, and tunicamycin (Fig. S1*D*). In this context, the mitochondrial CSE translocation observed in this study is not likely related to the altered ER stress level. On the other hand, the rates of $[Ca^{2+}]_i$ increase induced by A23187, thapsigargin, and tunicamycin are much slower and the elevated $[Ca^{2+}]_i$ levels persist much longer than those induced by phenylephrine (Fig. 3*C*), consistent with previously reported changes in calcium kinetics induced by A23187 (14), thapsigargin (15), tunicamycin (11), and phenylephrine (14). Thus, we reasoned that CSE mitochondrial translocation may be related to the kinetics and sustained increased levels of $[Ca^{2+}]_i$.

The requirement for CSE translocation to mitochondria to support ATP production under stress conditions may be unique to the cells whose metabolism relies on oxygen supply and oxidative phosphorylation and whose H_2S production is greatly dependent on CSE, such as vascular SMCs. On the other hand, CSE mitochondrial translocation in cancer cells might not be critically needed (Fig. S2*C*), given that most cancer cells rely on aerobic glycolysis for their energy supply (16). Furthermore, CSE is the only H_2S-producing enzyme in vascular SMCs, whereas in the human colon cancer cells (WiDr), both CSE and cystathionine β-synthase (CBS) play important roles in H_2S production (17). The presence of CBS in WiDr cells may compensate for the lack of CSE mitochondrial translocation in situations where mitochondrial ATP production is regulated by H_2S.

Mitochondrial constitutional proteins (~3,000) are mostly synthesized in the nucleus and exist in the cytosol as preproteins, except for 13 proteins synthesized inside mitochondria. The preproteins in their unfolded forms are recognized for their consensus motif or presequences represented by φXXφφ (where φ is a hydrophobic amino acid and X is any amino acid) by a group of at least six protein complexes, termed translocases, located in the outer and inner mitochondrial membranes (18). Translocases rapidly import preproteins into one of the four mitochondrial compartments—outer membrane, intermembrane space, inner membrane, and matrix (19)—where these preproteins are proteolytically processed to their mature forms. Translocases also provide translocation machineries for nonpreprotein molecules, such as tRNA (20) and heme oxygenase-1, which produces

carbon monoxide (21). The activities of translocases are dependent on ATP and/or matrix metalloproteinase (22). Among identified translocases, Tom complexes are located on the outer mitochondrial membrane.

In this study, we have demonstrated the existence of Tom20 (a 20-kDa translocase) in mitochondrial fractions of SMCs. After A23187 stimulation, the expression of Tom20 is significantly increased, and its coimmunoprecipitation with CSE on mitochondrial membranes is elevated. Previous molecular dynamics analyses identified a domain in the C-terminal of CSE (amino acids 384–394) and a domain in the N-terminal (amino acids 51–84) of Tom20, which form the first α-helix, as potential interaction interfaces for binding of Tom20 and CSE (23–28). This is consistent with previous reports of a grooved configuration formed by the first and third helixes of Tom20 that serves as the binding site for recognition of proteins bearing a signal motif, for example, the amino acid sequence 389–393 (leucine-aspartic acid-arginine-alanine-leucine) (29). The binding of Tom20 with CSE appears to be the prerequisite for CSE mitochondrial translocation. This conclusion is supported by two lines of evidence: the elimination of CSE translocation after knockdown of Tom20 expression and the enhancement of CSE translocation after Tom20 overexpression in SMCs.

Given that H_2S is relatively permeable to lipid bilayer, it may be asked why it matters whether or not CSE is translocated into mitochondria to produce H_2S there. There are several worthy possible answers to this intriguing question. As a reactive molecule, H_2S produced in the cytosol can be transformed, buffered, or scavenged before it diffuses into mitochondria to affect mitochondrial functions. H_2S production inside mitochondria near the microdomain where the electron transport chain and ATPase operate, would require that CSE and its substrate cysteine be inside the mitochondria. L-cysteine in mammalian cells is catabolized by one of two pyridoxal-5′-phosphate–dependent enzymes, CBS or CSE (30). Cysteine does not diffuse freely across the mitochondrial membrane; the concentration gradient for cysteine across the mitochondrial membrane is approximately three in SMCs under resting conditions. Previous studies also have reported that in liver mitochondria the cysteine level was about four times of that in the cytosol (31, 32).

Translocation of CSE into mitochondria helps reduce mitochondrial cysteine via desulfhydration reactions (33). Cysteine metabolites such as H_2S function as antioxidants (34). Pyruvate, another cysteine metabolite, is critical in supporting the mitochondrial electron transport chain and ATP production, and in reducing electron leakage. In the present study, we found that, in synchrony with the increase in H_2S level in mitochondria, A23187 stimulation decreased the cysteine content of mitochondria. This effect can be attributed to the catalyzing effects of mitochondrial CSE. In contrast, A23187 stimulation increased cytosolic cysteine content, possibly due to A23187-induced CSE overexpression. CSE also is responsible for converting cystathionine into cysteine in mammals (35). The A23187-decreased concentration gradient of cysteine across the mitochondrial membrane is a result of CSE translocation, as demonstrated by the complete disappearance of this gradient change in KO-SMCs, which lack CSE expression. Thus, CSE translocation to mitochondria under stressed conditions may play a crucial role in mitochondrial cysteine metabolism.

In the cardiovascular system, H_2S at physiological concentrations (i.e., low micromolars) mitigates ischemia/reperfusion injury by inhibiting inflammation and preserving mitochondrial functional and structural integrity (36). The present study elucidates one of the molecular mechanisms for H_2S-induced preservation of mitochondrial function. A previous study found that A23187 stimulates mitochondrial ATP production via increased activity of mitochondria-bound hexokinase (37). As shown here, A23187 also stimulates ATP production in part through mitochondrial translocation of CSE in vascular SMCs. The A23187-increased ATP production is reduced to the same degree in the PPG-treated WT-SMCS and in KO-SMCs without PPG treatment. These unique observations reaffirm a critical role of CSE translocation and involvement of CSE-generated H_2S in mitochondria in regulating energy metabolism. With hypoxia alone or NaHS application alone, ATP production from mitochondria is reduced. This reduction is not surprising, because it has been reported that H_2S decreases ATP content under normoxic condition (38). What is intriguing is that H_2S, either produced endogenously after A23187-stimulated CSE translocation or provided in the form of NaHS, reversed the hypoxia-repressed mitochondrial ATP production and decreased the ADP/ATP ratio (Fig. 5). The physiological relevance of this observation on the isolated mitochondrial preparation was validated using the cultured intact SMCs, in which NaHS also partially reversed hypoxia-inhibited ATP production (Fig. S2*D*). Our results suggest that H_2S may function as an energy substrate to sustain ATP production under stress conditions. In other words, in conjunction with hypoxia, H_2S may help produce more ATP. H_2S at toxic levels inhibits cytochrome *c* oxidase, a key component of the mitochondria respiratory complex IV (1). By doing so, it inhibits ATP production under normoxic conditions. The electrons generated from the oxidative phosphorylation pathway can be transported from quinone to cytochrome oxidase on their way to drive the synthesis of ATP. With a physiological level of H_2S, cytochrome *c* oxidase is not inhibited, and sulfide oxidation likely contributes to mitochondrial ATP production (39). With hypoxia, the electrons from sulfide can be injected into the mitochondrial electron transport chain, directed toward the reduction of malate to succinate by reversing the mitochondrial complex II (4). This bioenergetic process may be catalyzed by sulfide quinone reductase, which is linked to the electron transport chain (40).

In conclusion, we found that in response to elevated $[Ca^{2+}]_i$ level CSE can be translocated from the cytosol into mitochondria, aided by Tom20, in vascular SMCs. This leads to the metabolism of cysteine and production of H_2S inside mitochondria. As such, the conventional belief that H_2S in eukaryotes is produced only in the cytosol and consumed in mitochondria is incorrect. Furthermore, the notion that eukaryotes do not need H_2S in the energy metabolism process should be revised. In SMCs, mitochondrial CSE translocation and H_2S production confer resistance to hypoxia by increasing ATP synthesis. By sensing the oxygen levels in mitochondria, H_2S regulates ATP production under different conditions, thereby fulfilling the roles of an oxygen sensor (41) and a regulator of energy metabolism. These findings may help deepen and widen our understanding of fundamental sulfur metabolism and the regulation of mitochondrial energy metabolism in eukaryotes.

Materials and Methods

Cell Culture and Treatments. SMCs from mesenteric arteries of WT mice (WT-SMCs) or from CSE KO mice (KO-SMCs) were isolated and identified as described previously (42). For hypoxic conditions, cells or isolated mitochondria were exposed to hypoxia by incubating the preparations in an anaerobic chamber (Coy Laboratory Products) with a continuous flow of a humidified mixture of 1% O_2, 94% N_2, and 5% CO_2 gas to maintain the partial pressure of O_2 at 29.8 ± 1.5 mmHg (n = 8) at 37 °C, compared with 154 ± 8.8 mmHg (n = 8) for the media under nomoxic condition (5% CO_2 in room air). O_2 partial pressure of the media was measured using a Gem OPL CO-Oximeter (Premier 3000; Instrumentation Laboratory). Each measurement of O_2 partial pressure was repeated for at least four times.

Measurement of Mitochondrial H_2S Production Rate and H_2S Concentrations. Mitochondrial fractions were isolated and sonicated in 50 mM ice-cold potassium phosphate buffer (pH 6.8). H_2S production rate of sonicated mitochondria was measured as described previously (43). More details are provided in *SI Materials and Methods*.

Statistical Analysis. All data are expressed as mean ± SEM. Statistical analyses between two groups were performed using the unpaired Student t test.

Statistical analysis of more than two groups was performed using one-way ANOVA with Dunnett's multiple-comparisons post hoc test. A P value < 0.05 was considered statistically significant.

ACKNOWLEDGMENTS. This study was supported by a Natural Sciences and Engineering Research Council of Canada Discovery Grant (to R.W.). G.Y. is supported by a New Investigator award from the Heart and Stroke Foundation of Canada.

1. Blackstone EA, Morrison ML, Roth MB (2005) H_2S induces a suspended animation-like state in mice. *Science* 308:518.
2. Liu DK, Chang SG (1987) Kinetic study of the reaction between cystine and sulfide in alkaline solutions. *Can J Chem* 65:770–774.
3. Searcy DG (2003) Metabolic integration during the evolutionary origin of mitochondria. *Cell Res* 13:229–238.
4. Goubern M, Andriamihaja M, Nübel T, Blachier F, Bouillaud F (2007) Sulfide, the first inorganic substrate for human cells. *FASEB J* 21:1699–1706.
5. Verma G, Datta M (2010) IL-1beta induces ER stress in a JNK-dependent manner that determines cell death in human pancreatic epithelial MIA PaCa-2 cells. *Apoptosis* 15: 864–876.
6. Pace NR (1997) A molecular view of microbial diversity and the biosphere. *Science* 276: 734–740.
7. Ali H, et al. (1985) The ability of thapsigargin and thapsigargicin to activate cells involved in the inflammatory response. *Br J Pharmacol* 85:705–712.
8. Rogers TB, Inesi G, Wade R, Lederer WJ (1995) Use of thapsigargin to study Ca^{2+} homeostasis in cardiac cells. *Biosci Rep* 15:341–349.
9. Furuya Y, Lundmo P, Short AD, Gill DL, Isaacs JT (1994) The role of calcium, pH, and cell proliferation in the programmed (apoptotic) death of androgen-independent prostatic cancer cells induced by thapsigargin. *Cancer Res* 54:6167–6175.
10. Werno C, Zhou J, Brüne B (2008) A23187, ionomycin and thapsigargin upregulate mRNA of HIF-1alpha via endoplasmic reticulum stress rather than a rise in intracellular calcium. *J Cell Physiol* 215:708–714.
11. Bian ZM, Elner SG, Elner VM (2009) Dual involvement of caspase-4 in inflammatory and ER stress-induced apoptotic responses in human retinal pigment epithelial cells. *Invest Ophthalmol Vis Sci* 50:6006–6014.
12. Buckley BJ, Whorton AR (1997) Tunicamycin increases intracellular calcium levels in bovine aortic endothelial cells. *Am J Physiol* 273:C1298–C1305.
13. Belmont PJ, et al. (2008) Coordination of growth and endoplasmic reticulum stress signaling by regulator of calcineurin 1 (RCAN1), a novel ATF6-inducible gene. *J Biol Chem* 283:14012–14021.
14. Reinhart PH, Taylor WM, Bygrave FL (1983) The effect of ionophore A23187 on calcium ion fluxes and alpha-adrenergic agonist action in perfused rat liver. *Biochem J* 214:405–412.
15. Chew CS, Petropoulos AC (1991) Thapsigargin potentiates histamine-stimulated HCl secretion in gastric parietal cells but does not mimic cholinergic responses. *Cell Regul* 2:27–39.
16. Gatenby RA, Gillies RJ (2004) Why do cancers have high aerobic glycolysis? *Nat Rev Cancer* 4:891–899.
17. Cao Q, Zhang L, Yang G, Xu C, Wang R (2010) Butyrate-stimulated H2S production in colon cancer cells. *Antioxid Redox Signal* 12:1101–1109.
18. Kutik S, Guiard B, Meyer HE, Wiedemann N, Pfanner N (2007) Cooperation of translocase complexes in mitochondrial protein import. *J Cell Biol* 179:585–591.
19. Lithgow T, Glick BS, Schatz G (1995) The protein import receptor of mitochondria. *Trends Biochem Sci* 20:98–101.
20. Tarassov I, Entelis N, Martin RP (1995) An intact protein translocating machinery is required for mitochondrial import of a yeast cytoplasmic tRNA. *J Mol Biol* 245: 315–323.
21. Turkseven S, et al. (2007) Impact of silencing HO-2 on EC-SOD and the mitochondrial signaling pathway. *J Cell Biochem* 100:815–823.
22. Mokranjac D, Neupert W (2008) Energetics of protein translocation into mitochondria. *Biochim Biophys Acta* 1777:758–762.
23. Ding HQ, Karaswa N, Goddard WA (1992) Atomic level simulations on a million particles: The cell-multipole method for Coulomb and London non-bond interactions. *J Chem Phys* 97:4309–4315.
24. Ding H-Q, Karasawa N, Goddard WA (1992) The reduced-cell multipole method for Coulomb interactions in periodic systems with million-atom unit cells. *Chem Phys Lett* 196:6–10.
25. Jain A, Vaidehi N, Rodriguez G (1993) A fast recursive algorithm for molecular dynamics simulation. *J Comp Physiol* 106:258–268.
26. Mathiowetz AM, Jain A, Karasawa N, Goddard WA, 3rd (1994) Protein simulations using techniques suitable for very large systems: The cell multipole method for nonbond interactions and the Newton–Euler inverse mass operator method for internal coordinate dynamics. *Proteins* 20:227–247.
27. Vaidehi N, Jain A, Goddard WA (1996) Constant temperature-constrained molecular dynamics: The Newton–Euler inverse mass operator method. *J Phys Chem* 100: 10508–10517.
28. Lim KT, et al. (1997) Molecular dynamics for very large systems on massively parallel computers: The MPSim program. *J Comput Chem* 18:501–521.
29. Saitoh T, et al. (2007) Tom20 recognizes mitochondrial presequences through dynamic equilibrium among multiple bound states. *EMBO J* 26:4777–4787.
30. Wang R (2002) Two's company, three's a crowd: Can H_2S be the third endogenous gaseous transmitter? *FASEB J* 16:1792–1798.
31. Yao WB, Zhao YQ, Abe T, Ohta J, Ubuka T (1994) Effect of *N*-acetylcysteine administration on cysteine and glutathione contents in liver and kidney and in perfused liver of intact and diethyl maleate-treated rats. *Amino Acids* 7:255–266.
32. Ubuka T, et al. (1992) L-Cysteine metabolism via 3-mercaptopyruvate pathway and sulfate formation in rat liver mitochondria. *Amino Acids* 2:143–155.
33. Stipanuk MH, Dominy JE, Jr., Lee JI, Coloso RM (2006) Mammalian cysteine metabolism: New insights into regulation of cysteine metabolism. *J Nutr* 136(6 Suppl):1652S–1659S.
34. Yan SK, et al. (2006) Effects of hydrogen sulfide on homocysteine-induced oxidative stress in vascular smooth muscle cells. *Biochem Biophys Res Commun* 351:485–491.
35. Greenberg DM (1975) Biosynthesis of cysteine and cystine, *Metabolic Pathways*, ed Greenberg DM (Academic, New York), Vol 7, 3rd Ed, pp 505–528.
36. Elrod JW, et al. (2007) Hydrogen sulfide attenuates myocardial ischemia-reperfusion injury by preservation of mitochondrial function. *Proc Natl Acad Sci USA* 104:15560–15565.
37. Glass-Marmor L, Penso J, Beitner R (1999) Ca^{2+}-induced changes in energy metabolism and viability of melanoma cells. *Br J Cancer* 81:219–224.
38. Nicholson RA, et al. (1998) Inhibition of respiratory and bioenergetic mechanisms by hydrogen sulfide in mammalian brain. *J Toxicol Environ Health A* 54:491–507.
39. Lagoutte E, et al. (2010) Oxidation of hydrogen sulfide remains a priority in mammalian cells and causes reverse electron transfer in colonocytes. *Biochim Biophys Acta* 1797:1500–1511.
40. Hildebrandt TM, Grieshaber MK (2008) Three enzymatic activities catalyze the oxidation of sulfide to thiosulfate in mammalian and invertebrate mitochondria. *FEBS J* 275:3352–3361.
41. Olson KR, et al. (2008) Hydrogen sulfide as an oxygen sensor in trout gill chemoreceptors. *Am J Physiol Regul Integr Comp Physiol* 295:R669–R680.
42. Yang G, et al. (2010) Cystathionine gamma-lyase deficiency and overproliferation of smooth muscle cells. *Cardiovasc Res* 86:487–495.
43. Zhao W, Zhang J, Lu Y, Wang R (2001) The vasorelaxant effect of H(2)S as a novel endogenous gaseous K(ATP) channel opener. *EMBO J* 20:6008–6016.